A transferable method for the automated grain sizing of river gravels

David J. Graham, Stephen P. Rice and Ian Reid

Department of Geography, Loughborough University, Loughborough, Leicestershire, LE11 3TU UK.

INDEX TERMS: 1824 Hydrology: Geomorphology; 1860 Hydrology: Runoff and streamflow; 1894 Hydrology: Instruments and techniques; 1224 Geodesy and gravity: Photogrammetry.

KEYWORDS: grain-size distribution, grain-size analysis, digital imagery, fluvial geomorphology, image processing, sediments.

The spatial and temporal resolution of surface grain-size characterization is constrained by the limitations of traditional measurement techniques. In this paper we present an extremely rapid image-processing-based procedure for the measurement of exposed fluvial gravels and other coarse-grained sediments, defining the steps required to minimize the errors in the derived grain-size distribution. This procedure differs significantly from those used previously. It is based around a robust object-detection algorithm that produces excellent results on images exhibiting a wide range of sedimentary conditions, crucially, without any user intervention or site-specific parameterization. The procedure is tested using a dataset comprising 39 images from three rivers with contrasting grain lithology, shape, roundness and packing configuration and representing a very wide range of textures. It is shown to perform more consistently than the best existing automated method, achieving a precision equivalent to that obtainable by Wolman sampling, but taking between one sixth and one twentieth of the time. The error in area-by-number grain-size distribution percentiles is typically less than 0.05 ψ.

1. Introduction

The spatial variability of grain size at a variety of scales makes the characterization of fluvial sediment notoriously difficult [*Church et al.,* 1987; *Wolcott and Church,* 1991]. Large sample sizes are necessary to ensure adequate representation of the population and sampling is therefore time-consuming, laborious and costly. Conventional sampling techniques leave potentially important textural variations unresolved in hydraulic, geomorphological and ecological studies of river channel behavior.

The development of sampling techniques that achieve satisfactory characterization of grain size whilst simultaneously reducing the time spent in both the field and the laboratory is highly desirable. Several researchers have used emulsion-based photographic data capture to reduce field time [*Adams,* 1979; *Church et al.,* 1987; *Rice and Church,* 1998], but subsequent analysis of the photographs can be extremely time-consuming. Even the most advanced of such procedures, photo-sieving [*Ibbeken and Schleyer,* 1986; *Diepenbroek et al.,* 1992; *Diepenbroek and De Jong,* 1994; *Ibbeken et al.,* 1998], relies on manual identification and digitization of individual particle boundaries.

These limitations can be overcome using automated methods of extracting information from images. Such methods have been used extensively in biomedical applications, which have driven much of the research on image segmentation and measurement [*Bankman,* 2000], and have been used widely in the Earth sciences [*Ghalib and Hryciw,* 1999; *Franciskovic-Bilinski et al.,* 2003; *Posadas et al.,* 2003; *Perring et al.,* 2004] and civil engineering [*Alshibli and Alsaleh,* 2004; *Wettimuny and Penumadu,* 2004].

River beds present a particularly complex problem because grains are highly variable in shape and may be partially hidden or inclined relative to the plane of the image, there may be significant heterogeneity in hue and grain-surface texture between and within individual grains, and the surface has elevation variations which may result in uneven lighting and shading across individual grains and across the image. Nevertheless, recent years have seen several groups attempt to characterize automatically from digital images the surface grain-size distribution of fluvial gravels exposed above the water surface. *McEwan et al.* [2000] used an image-processing method to extract information from high-resolution digital-elevation models generated using a laser scanner and suggested that a similar approach may be applied to photographic images. *Butler et al.* [2001] and *Reid et al.* [2001] have presented encouraging results for small numbers of such images collected under controlled conditions. *Sime and Ferguson* [2003] have demonstrated the application of an automated procedure using 12 sets of images and associated control data from the Vedder River, Canada, and *Carbonneau et al.* [2004] have used a different approach based on empirical relations between grain size and the semivariance characteristics of aerial photographs to derive an almost continuous characterization of grain size along 80 km of the Sainte-Marguerite River, Canada. Although these results are encouraging, the test data sets used were small and/or limited to individual rivers and the transferability of such approaches to a range of lithotypes, grain shapes, packing configurations and sizes is, as yet, unproven.

The challenge now is to design a transferable procedure that performs well under a range of sedimentary and sampling conditions so that image-processing-based methods of grain-size measurement can be widely adopted. Here we present a new procedure for exposed gravel surfaces and demonstrate its performance using a test dataset that is three times larger and exhibits a wider range of textural variability than has previously been presented. The test data were collected from

three different field sites with contrasting grain lithologies and characteristic grain shape and roundness. The key benefit of this work is that the extensive test dataset, combined with the rigorous testing procedures we have adopted, gives us confidence that the procedures adopted are robust and transferable between field sites with diverse physical characteristics without the need for re-parameterization to optimize their performance under different conditions.

In a companion paper [*Graham et al.,* 2005], we isolated a preferred object-recognition algorithm that minimizes image-processing errors. This was achieved by comparing 16224 segmented images derived from 416 different procedures or variants thereof against manually digitized grain boundaries from our set of field images. A key objective of the paper was that the selected procedure should perform well across images derived from a range of lithological provinces and not be tailored to any particular river or set of sedimentary circumstances. The procedure that we prefer does not necessarily achieve the best possible result at every individual site, but it does perform best overall and it represents a robust compromise that successfully mimics the boundary identification of a human operator across a very wide range of sediment textures and lithologies. Here, our focus is on deriving useful grain-size information from images of gravel beds. We describe an automated grain-sizing (AGS) method and assess its performance by comparing estimated grain-size percentiles and the underlying fractional grain counts with those determined by manual methods for the same sediment patches. A unique feature of this assessment is that the data sets were obtained from three rivers selected for the contrasting lithologies of their bed materials.

2. Recommended automated grain-sizing procedure

The automated procedure is divided into four keys stages: (i) image collection; (ii) image pre-processing; (iii) image processing and analysis; and (iv) the derivation of a grain-size distribution (Figure 1). The procedure has been designed with ease-of-use as a guiding principle, such that it is simple and rapid to employ without the need for specialist equipment or extensive technical knowledge. For this reason, the method can use a relatively inexpensive, compact, digital camera held in the hand, and employs single images rather than stereo pairs. The procedure is facilitated by software we have developed using Matlab® (see http://www.lboro.ac.uk/research/phys-geog/ for further information).

2.1. Image collection

Data input to the procedure is an image of a patch of sediment collected approximately vertically with a digital camera. The scale of the image should be such that the smallest grain of interest has a *b*-axis (the minor axis in the imagery) larger than 23 pixels [*Graham et al.,* 2005]. This relation may be expressed as

$$A = \left(\frac{g\sqrt{P}}{23000} \right)^2$$

where A is the area photographed (m^2), g is the *b*-axis of the smallest grain of interest (mm) and P is the number of pixels in the image (which may not be identical to the number of pixels quoted on the camera body and in advertising).

Reference points must be placed at each corner of the rectangular sample patch to provide a scale and define the boundary of the patch in the image. In practice, the easiest means of achieving this is by the use of a slightly oversized wooden frame with protruding metal wires, the tips of which locate the patch corners (Figure 2). Any grains that lie along the edge of the patch must be entirely contained within the image. For best results, the patch should be shielded from direct sunlight and lit from above with a camera-mounted flash.

2.2. Image pre-processing

Color information is not required and increases processing times, so the first step is to convert the image to grayscale (intensity). The use of a complete lens-distortion model, usual in photogrammetric applications, is not feasible for compact cameras with a zoom lens. However, it is possible to derive an approximate correction for radial distortion, which is by far the most significant of the lens distortions in non-metric cameras [*Dymond and Trotter,* 1997; *Wolf and Dewitt,* 2000; *Zhang,* 2000]. Radial distortions vary as a function of distance from the image center and radial displacement can be represented by an odd-quintic polynomial [*Schenk,* 1999]. Providing that a consistent area is photographed from approximately the same height, so keeping the focal length approximately constant, this displacement function may be used to derive a suitable correction for a particular camera (http://www.lboro.ac.uk/research/phys-geog/). For the camera and setup used in this study, the application of a radial lens correction resulted in a small, but statistically insignificant, error reduction in the derived grain-size distribution. Because the general applicability of this result to different lenses and field configurations is uncertain, and the correction is straightforward and easily obtained, it is recommended that the correction should be applied. However, the consequences of not doing so are unlikely to be critical.

Finally, the image is corrected for the perspective effect resulting from the fact that the principal point, center of the sample patch and nadir may not be coincident. To accomplish this, the locations of the four reference points are identified and mapped onto a rectangle with the correct aspect ratio using a projective transform and bilinear interpolation. The mean pixel size is maintained at approximately the same scale during this transformation, and the interpolation results in no appreciable degradation in image quality.

2.3. Image processing and analysis

The optimal image processing and analysis procedure for this application was selected after rigorous assessment of four procedures using 416 permutations of the internal parameters. Only a brief treatment of the optimal procedure is given here and the reader is referred to *Graham et al.* [2005] for a full discussion.

The image is first manipulated by the application of a median filter which smoothes markings on the grain surfaces whilst preserving edges [*Russ,* 1999]. Interstices are then enhanced by the application of a morphological bottom-hat transform. A first segmentation is obtained using an adaptive double-threshold approach in which the threshold levels are defined in terms of percentiles in the image-intensity frequency distribution, and this is then refined using a watershed segmentation algorithm with minima suppression (Figure 3). The segmented images should be checked at this stage in case the segmentation has failed for some reason.

Using the reference points that define the corners of the rectangular sample patch in the image, those objects that lie within the patch are selected for measurement. Because large grains

occupy more space than smaller ones, the inclusion of every grain intersecting the edge of the sample patch would lead to a coarsening of the observed size distribution. To remove this bias, all objects intersecting the top and left edges of the sample patch are included and those intersecting the bottom and right edges excluded. The selected objects are measured using an ellipse-fitting procedure to obtain the minor axis (approximating the *b* or intermediate axis in conventional granulometry). *Graham et al.* [2005] have demonstrated that this approach gives an unbiased estimate of the minor-axis length. The number of pixels in each object is also recorded as a measure of object area.

2.4. Derivation of a size distribution

At the completion of the image processing and analysis stage, a list of *b*-axis lengths and corresponding areas for each of the identified objects in the image is obtained, measured in pixels. These must be converted into metric units. This is simple given the known parameters of the projective transform applied in the pre-processing stage.

If a size distribution that is directly comparable to sieve-derived data is required, the grain *b*-axes can be modified using a sieve-correction factor $D_s / b = 0.707\left[1 + (c/b)^2\right]^{0.5}$ [*Church et al.,* 1987], where the ratio of square-hole sieve size and true *b*-axis (D_s/b) is related to flatness (c/b). This relation accounts for the influence of flatness in determining whether a particle is able to pass through a square-hole sieve. In effect, the conversion adds an artifact (error) to the data, but nevertheless facilitates the direct comparison of image-processing-derived and sieve- or template-based grain-size distributions. Since the flatness of individual grains in the image is unknown, an average value that has been obtained manually for the site can be used, but testing indicates that the derived grain-size distribution is relatively insensitive to the flatness index, even when there is an obvious difference in average grain shape (http://www.lboro.ac.uk/research/phys-geog/). This suggests that use of a single average flatness index is unlikely to introduce a significant bias to the grain-size distributions for most lithologies. It should be necessary to survey the flatness index only if the sediment is characterized by exceptionally platy or equant grains, otherwise we recommend the use of a sieve-correction factor of 0.79 (corresponding to a flatness index of 0.51). An exception to this may be where there is a marked variation in grain shape with size.

The sieve-corrected or uncorrected *b*-axes measurements may be used directly to generate a cumulative area-by-number grain-size distribution, which is directly comparable to a paint-and-pick sample. Alternatively, it is simple to obtain a grid-by-number equivalent sample (comparable to a Wolman sample) by: (i) sorting the *b*-axis measurements into size classes and summing the total area within each class; (ii) using the method of *Sime and Ferguson* [2003]; or (iii) applying an appropriate transformation to the area-by-number data [*Kellerhals and Bray,* 1971].

3. Procedure evaluation

3.1. Test data sets

Fieldwork was undertaken at three sites chosen because of their distinct lithologies and associated differences in grain shape, roundness and packing configuration (Figure 4). The sites were not intended to represent the full range of conditions that may be encountered, but their

contrasting physical properties were designed to be a harsh test of the automated procedure's ability to determine the grain-size distribution without the need for re-parameterization. The bed sediments of Ettrick Water, Scotland, are characterized by speckled, pale-colored clasts of grit and shale, that tend to be equant and sub-angular to sub-rounded. The Afon Ystwyth, Wales, is dominated by clasts of fine-grained grit, dark in color and commonly platy in shape. The bed material of the River Lune, England, consists of very pale limestone clasts mixed with a scattering of darker sandstone clasts, which are predominantly equant and rounded.

A total of 39 sediment patches were selected across the three sites to represent a wide variety of grain-size distributions (Table 1; Figure 5). The samples included both open- and closed-framework gravels, and the proportion of fines (less than 8 mm) was up to 53% with an average of 9%. Each patch was rectangular with an area of 1.2 m^2, the aspect ratio reflecting that of the images recorded by the camera (4:3).

The collection procedure for the test images was more involved than the procedure we recommend for routine operations, for which the camera can be held in the hand at a suitable height and with the lens axis approximately vertical. A wooden frame was placed over each sample patch to ensure selection of a consistent area and the corners were marked using 10 mm diameter adhesive survey targets. The frame was then removed and the patch was photographed using an inexpensive compact digital camera (an Olympus C-3030Z with a FL-40 external flash; 2048 by 1536 maximum image resolution; rapid advances in technology mean that modestly priced cameras with a higher resolution are now available). Images were stored in JPEG format using the minimum compression supported by the camera, resulting in image sizes of 1.5 – 2 MB with no apparent loss in image quality when compared visually with an uncompressed image (TIFF format, 9 MB). The use of JPEG images does not affect the quality of the derived size information because most of the compression is associated with the hue and saturation information, whilst the automated grain-sizing procedure only uses the intensity component. Photographs were taken vertically from a gantry at a height of 1.5 m, giving a pixel resolution of approximately 0.7 mm on the ground (Figure 6a). This height minimized barrel distortion associated with the use of a wide-angle lens whilst still making the camera easily accessible from the ground. Images were collected in a variety of natural and artificial lighting conditions (natural overcast and sunlit, artificially shaded, direct and bounced flash) in order to determine optimum illumination.

To facilitate calibration and evaluation of the automated grain-size characteristics, the paint-and-pick procedure [*Lane and Carlson,* 1953] was used to define the 'true' grain-size distribution of each sample patch. The most common method of characterizing the size distribution of a sediment surface, the Wolman sample [*Wolman,* 1954], was inappropriate because the grain-independence criterion cannot be met at such small scales. The frame was re-laid over the patch to define the area and the patch sprayed with aerosol paint. Painted grains larger than 4 mm were collected and returned to the laboratory (Figure 6b). The three orthogonal axes of those grains that were too large to be returned easily to the laboratory were measured in the field with a rule. To facilitate comparison between the data derived from the image processing and the paint-and-pick sampling, a method analogous to that used in the image-analysis procedure was used to select the grains on the edges of the sampled area. All grains intersecting the top and left edges of the patch were collected and those intersecting the bottom and right edges discarded.

To characterize grain shape on each river, approximately 500 clasts were selected on a regular grid (node spacing greater than $2D_{max}$) from the facies that had been sampled photographically and their three orthogonal axes measured and recorded to the nearest 5 mm. There were no significant variations in shape across the sampled surfaces. The mean flatness at each site (the ratio of the short

and intermediate axes) and the associated square-hole sieve correction factors are presented in Table 2.

Digital photographs were processed using the automated grain-sizing procedure outlined above, including the square-hole sieve correction (with a site-specific correction factor). The grain-size distributions were truncated at 4 ψ (psi = -phi = $\log_2$ mm) (corresponding to about 23 pixels in the original images). Two patches were rejected (one each from the Afon Ystwyth and Ettrick Water) as a result of poor image segmentation and excluded from further analysis [*Graham et al.,* 2005]. These failures resulted from a combination of the presence of very fine sediment, significant chromatic aberration and slight optical vignetting. The paint-and-pick grains were sieved at 0.5 ψ intervals with square-hole sieves. Grains that were too large for the sieves were sorted into size fractions using a square-hole template. The grains in each fraction were counted manually. To make them consistent with the sieved sediment, those large grains measured with a rule in the field were converted to sieve-equivalent sizes using the correction equation and then combined with the sieve-derived data. In total, this correction was applied to only 1.3% of the grains at a single site (Ettrick Water). Hereafter, those data derived by the automated grain-sizing (AGS) procedure are referred to as AGS data, and those derived by sieving the grains obtained by paint-and-pick sampling are referred to as sieve data.

Percentiles (ψ_x) of the area-by-number AGS data are derived directly from the list of *b*-axis lengths without the need for interpolation. Percentiles of the sieve data and grid-by-number equivalent AGS data are derived using a spline interpolation between 0.5 ψ size-class boundaries in the cumulative frequency distribution, providing a more precise estimate of the true percentile value than the more usual linear interpolation (http://www.lboro.ac.uk/research/phys-geog/).

3.2. AGS procedure performance

Because the grains of the sieve control data were collected using an area-by-number method (paint-and-pick sampling), the resulting grain-size distributions are directly comparable to the area-by-number AGS data derived directly from the measured grain *b*-axes. It is possible to convert the sieve data to a grid-by-number equivalent by applying the conversion of *Kellerhals and Bray* [1971] and comparing these with the AGS data in grid-by-number form. However, because the conversion uses an exponent of 2, it magnifies the relative size of any errors in the coarse part of the grain-size distribution. For this reason, the primary and more appropriate test of the AGS procedure is on an area-by-number basis.

The success of the AGS procedure at replicating the grain-size percentiles derived from the sieve data is illustrated in Figure 7a for each of the three field sites and for seven of the most commonly used percentiles ($\psi_{5,\ 16,\ 25,\ 50,\ 75,\ 84,\ 95}$) [following the method of *Reid et al.,* 2001]. *Sime and Ferguson* [2003] assessed the performance of their image-processing procedures by calculating the errors associated with these seven percentiles. They defined the mean error (or procedure bias) as $b = \frac{1}{n}\sum(\psi_s - \psi_{AGS})$ and the mean-square error as $E_{ms} = \frac{1}{n}\sum(\psi_s - \psi_{AGS})^2$, where ψ_s and ψ_{AGS} are the sieve- and AGS-derived percentile values, respectively, and *n* is the sample size (the number of patches multiplied by the number of percentiles used). The irreducible random error *e* of the estimates is then $e^2 = E_{ms} - b^2$. Using this approach, the irreducible random error is represented in Figure 7a by the scatter around a line offset from the line of equality by the procedure bias.

The approach described above assumes that bias is independent of percentile. This is shown not to be true in Figure 7b, which illustrates the errors associated with every percentile between 1

and 99. The heavy line represents the bias for each percentile (termed the percentile bias to differentiate it from the procedure bias). The percentile bias is generally close to zero at low percentiles, positive at high percentiles, and slightly negative for intermediate percentiles. The largest errors are associated with the highest percentiles and probably result from the splitting of some of the largest grains by the watershed segmentation algorithm. For most percentiles at the Afon Ystwyth and Ettrick Water, the percentile bias is not significantly different from zero with 95% confidence (Figure 7b, Table 3). There is a small but significant bias for most low percentiles in the case of the River Lune.

The percentile-based assessment of the AGS procedure is useful because percentiles are the conventional method of representing grain-size distributions. However, this assessment is incomplete because it does not directly assess the ability of the AGS procedure to measure individual grains correctly. This approach may hide variations in performance that are size dependent rather than dependent on position within the grain-size distribution. One means of assessing this is to examine the number of grains in individual sieve fractions. Figure 8 illustrates the number of grains in 0.5 ψ size fractions of the sieve data compared with equivalents of the AGS data. Two features of interest emerge. First, the amount of scatter is greater than that associated with the percentile plots, although the scatter in the largest sizes is likely to reflect the very small number of grains involved. Second, there is underestimation of the number of grains in all size classes. In general the AGS procedure identifies about half of the grains in the sieve sample. In previous work, only *Butler et al.* [2001] have reported the number of grains identified, and they too observed a significant depletion in the number identified by their automated procedure. However, despite this undercounting, the precision of the percentile values is excellent because the depletion is consistent across size classes. The potential sources of this undercount are discussed in section 4.

3.3. AGS procedure performance compared to the Sime and Ferguson procedure

It is useful to compare the performance of the AGS procedure presented here with the best-performing procedure (aggregate method) of *Sime and Ferguson* [2003] when applied to the same set of images. Sime and Ferguson's results were presented as grid-by-number distributions, equivalent to Wolman samples. So, in order to facilitate direct comparisons, the results of our AGS procedure were converted to grid-by-number distributions by the application of a Kellerhals and Bray conversion. This approach was selected in preference to a direct measurement of the total area within each size class because it is the same conversion as that applied to the sieve control data, against which the performance of each of the two automated procedures is assessed.

The uncertainty associated with the use of the *Sime and Ferguson* [2003] method is comparable to that of their published result for their analyses of images collected in the Vedder River, with a mean irreducible random error of 0.27 ψ for all the sediment patches of the three UK sites, although the mean bias is less than half, at –0.42 ψ (Table 4). In contrast, the procedure developed here achieved a mean irreducible random error of 0.18 ψ and a mean bias of 0.14 ψ across the same three sites.

An investigation of the cause of the poorer performance of the *Sime and Ferguson* [2003] method led us to the conclusion that their published computer code contains an error in the way that it calculates the grid-by-number grain-size distribution after each grain has been identified and measured. Modifications to their code in order to obtain area-by-number data and to transform this into the equivalent of a grid-by-number sample using a Kellerhals and Bray conversion (as distinct from their method) resulted in a significant reduction in both the magnitude of the mean bias and the irreducible random error (Table 4). That the difference results from an error in the code of Sime

and Ferguson was confirmed by using a third method to derive a grid-by-number distribution (i.e. sorting the *b*-axis measurements into size classes and summing the total area within each class). This gave very similar results to those derived from the Kellerhals and Bray conversion. It is recommended, therefore, that the error analysis presented by *Sime and Ferguson* [2003] be approached with circumspection.

Comparison of the results of the corrected *Sime and Ferguson* [2003] method shows that their procedure outperforms the AGS procedure developed here by a small margin in the case of the River Lune, it produces similar results for the Afon Ystwyth, but comparatively poor results for the Ettrick Water. Where their procedure outperforms the AGS procedure, the grains are similar in shape and roundness (but not lithology) to those in the Vedder, for which their procedure was developed [*Sime and Ferguson,* 2003]. The strength of the AGS procedure is that it is not optimized for any particular set of circumstances; rather, it is designed to perform well at rivers with contrasting grain lithology, shape and roundness without re-parameterization, and this is reflected in its more consistent performance across the images from the three UK rivers. Furthermore, the test images used in this study were collected under conditions designed to minimize the effects of perspective and radial lens distortion and it is likely that the procedure of *Sime and Ferguson* [2003] – which does not include corrections for these effects – would perform less well on images collected under less well-controlled conditions.

3.4. AGS procedure performance and efficiency compared to Wolman sampling

There is a very limited literature on the precision that may be expected of conventional manual approaches to measuring surface grain-size distributions. *Rice and Church* [1996] used a bootstrapping approach to assess whether randomized grid-by-number (Wolman) samples match the population size distribution of well-sorted gravels on two Canadian rivers. They found that errors are percentile dependent but, when averaged for the two sites, they range between ±0.2 ψ and ±0.5 ψ (±0.2 ψ for ψ_{50}) for a 100-grain Wolman sample (the most commonly used sample size). *Green* [2003] obtained comparable results, but found that precision decreased markedly above the 90th percentile. Although these results are for only a limited number of sites, they indicate the magnitude of the error that may be expected for individual estimates of population percentiles. A reasonable requirement for the AGS size distributions is that the errors for individual samples should be comparable to the expected precision of a 100-grain Wolman sample. This is indeed the case, although the errors appear to be distributed differently across the percentiles.

Whilst the precision associated with the AGS procedure appears similar to that achievable by conventional measurement methods, the AGS approach has some significant advantages over conventional manual sampling in terms of errors. First, a Wolman sample requires a large sampling area, which may introduce bias by incorporating more than one facies, each of which can be sampled separately using the AGS procedure. Second, the AGS approach is not subject to operator error [*Marcus et al.,* 1995; *Bunte and Abt,* 2001]. Such errors will tend to increase the statistical errors quoted by *Rice and Church* [1996]. Third, the rapidity of the AGS procedure means that numerous measurements of grain-size distribution may be made *within* each facies, facilitating the averaging of percentile estimates to give greater confidence in their precision. This will have the additional advantages of increasing the sample size, reducing the error associated with inadequate sampling of the population, and facilitating the spatial mapping of grain size over small areas, which is important for understanding the development of some facies.

The time taken to complete a 100-grain Wolman sample is at least 0.5 person hours, and may be up to 2 person hours depending on the size and structure of the bed material. In contrast, our

recommended image-collection procedure, using a hand-held camera and a simple frame to define the sampling area, takes less than three minutes per image. The computer-processing time taken to derive a grain-size distribution from each image is about 2 minutes, plus 20 seconds of operator intervention to identify the reference points. The total time taken is, therefore, between one sixth and one twentieth of that required to undertake an equivalent Wolman sample. These efficiency gains will very rapidly recoup the capital cost of equipment. They will also enable grain-size information to be collected at a spatial and temporal resolution that has never before been achievable, whilst resulting in no damage to the surface being studied – a significant benefit in bed material monitoring and ecological studies. The detailed analysis that we have undertaken provides a robust indication of the type and magnitude of the errors that may be expected when using the AGS procedure. However, it would be prudent, especially where large numbers of samples are collected, to collect some control data in order to quantify errors that might arise from local factors e.g. unusual grain petrology and its effect on image segmentation.

4. Sources of error

4.1. Errors associated with the AGS procedure

Whilst the AGS procedure has been designed to minimize errors and maximize its transferability between different field sites, some errors remain. These may be divided into three types: (i) *image-processing errors* associated with the identification and measurement of grains in an image; (ii) *spatial distortions* resulting from the projection of a three-dimensional surface onto a two-dimensional plane through an imperfect lens; and (iii) *fabric errors* associated with the complex three-dimensional structure of exposed fluvial sediments.

There are two principal image-processing errors. The first results from the nature of the sediment at the time the photographs were taken. The surfaces of larger grains dry most quickly after rain or flood, leaving the interstices wet. Damp fine grains, located in the interstices between larger grains, may be lost to the image-processing procedure because there is insufficient tonal variation across them. The second problem is associated with the image-processing procedure itself. This may either merge grains or split individual grains, resulting in coarsening and fining of the size distribution respectively. These effects are discussed in *Graham et al.* [2005] and result from both incomplete segmentation and over-segmentation by the watershed procedure.

The errors associated with spatial distortions are likely to be small because the images have been corrected for tilt and the most significant lens distortion – radial distortion. There may be small errors associated with these distortions and with relief distortion. Correction for relief distortion would require the generation of a high-resolution digital-elevation model of the sample patch, a time-consuming and relatively complex procedure, the deployment of which would negate the benefits of a photographic approach to grain-size measurement. Provided that the camera height is large relative to the relief within the image, the effects of relief distortion will be small. This conclusion is supported by *Butler et al.* [2001] who found no significant difference between grain-size distributions derived from images corrected for relief distortion and those for which no correction was made.

Photographic approaches to grain-size measurement are fundamentally limited in that they can only measure what is seen by the camera. We use the term *fabric errors* to represent those errors that result from the inclination of individual grains relative to the plane of the image (leading

to a reduction in their apparent size) and the partial hiding of grains by others. Extreme examples of the latter we term *icebergs* because a grain may be almost entirely buried. Even if the AGS procedure measured the apparent size of every grain in the image without error, the derived grain-size distribution would be biased relative to the true distribution. It is widely recognized that fabric errors occur and are likely to vary between sites as a result of differences in imbrication angle and particle form [*Adams,* 1979; *Butler et al.,* 2001; *Sime and Ferguson,* 2003]. It is likely that much of the apparent difference between the procedure and percentile biases observed for the three sites studied here (Figure 7) result from these site-specific fabric errors. It may be possible to develop a correction based on direct measurements of imbrication angles and particle form and we will address this elsewhere. Even without this correction, the area-by-number percentile biases are not significantly different from zero for most percentiles at two of the sites, and, for the third site, they are less than 0.05 ψ (Table 3). For the largest percentiles, it may be desirable to correct for the mean deviation and an adjustment of about 0.1 ψ would be appropriate for the ψ_{95} at all three sites.

4.2. Errors associated with control sieve data

In addition to the errors associated with the AGS procedure itself, there are potential errors associated with the control data. In principle, a paint-and-pick sample should give a definitive assessment of the grain-size distribution of the sample patch for which it is collected. However, experience suggests that there are three potentially significant errors. In openwork gravels there may be penetration of paint into the interstices [*Church et al.,* 1987] so that a small proportion of subsurface grains may be inadvertently incorporated into the sample. Second, there are errors at the margin of the patch associated with paint drift, even if a frame with a masking skirt is used to delimit the patch boundary. This makes the patch boundary 'fuzzy' and may result in operators collecting a few additional grains. It is likely that the extra grains counted as a result of these two factors explain some of the apparent undercounting of grains by the AGS procedure. Third, where the paint-and-pick data are converted to a grid-by-number size distribution (from an area-by-number distribution) using a *Kellerhals and Bray* [1971] D^2 transformation, any errors or bias in the coarse fractions are magnified.

4.3. Errors associated with non-optimal lighting

To evaluate the effect of lighting on the derived grain sizes, each of the test patches were photographed under a range of natural and artificial lighting conditions. Tests indicated that optimal results are achieved when each patch is shaded from direct sunlight and lit from above by flash. Direct sunlight casts deep shadows, resulting in the measurement of brightly lit areas rather than grains. For sunlit images, irreducible random errors (for area-by-number data) were increased by between two and six times compared to results from images collected under controlled lighting conditions. The bias for individual percentiles was increased markedly for the River Lune and Ettrick Water, and, for the Afon Ystwyth, the standard errors were increased by up to 30 times. Overhead flash enhances the contrast between grains and interstices and images collected without flash exhibited significantly larger errors. The bias for individual percentiles was as much as 0.5 ψ and standard errors were commonly increased by 10 times. The irreducible random errors were increased by between 3 and 7 times for individual rivers. These results indicate that lighting conditions are critical if reliable results are to be achieved.

5. Conclusion

This paper has used the object-recognition procedure of *Graham et al.* [2005] to develop an automated grain-sizing procedure for exposed fluvial gravels based on the analysis of digital photographs. The procedure is simple and quick to employ using software that we have developed. It has been tested across a diverse range of textures at three field sites with contrasting bed sediment lithology, shape, roundness and packing configuration. The procedure is shown to perform more consistently than the best existing automated method. The precision achieved is comparable to that associated with conventional grid-by-number (Wolman) samples, but sampling takes between one sixth and one twentieth of the time. The key benefit of this work is that the extensive test dataset, combined with the rigorous testing procedures we have adopted, give us confidence that the procedure is robust and transferable between field sites with diverse physical characteristics without the need for re-parameterization to optimize performance in different circumstances.

Despite the impressive performance of the procedure, grain undercounting is apparent. Crucially, this undercounting does not result in a systematic bias in the derived grain-size distributions because the depletion is size-independent. There are also errors in the grain-size distributions that result from the inability of a photographic procedure to fully capture the three-dimensional nature of a sediment surface. These fabric errors are widely recognized in the literature, but do not appear to be large. Even without correcting for these effects, the bias in most individual area-by-number percentiles is less than 0.05 ψ; even for the coarsest percentiles the bias is only about 0.1 ψ (Table 3).

The automated grain-sizing procedure enables the collection of textural information at a temporal and spatial resolution that has never before been possible. It has the potential to facilitate advances in fluvial hydraulics by enabling the high-resolution parameterization of bed roughness. It enables frequent monitoring of bed-material size without destroying the surface under investigation, a particular concern in ecological studies. Field and computer-processing procedures have been simplified, enabling data to be collected and processed by operators with limited training.

The procedure tested here has been developed for sediment exposed above the water surface, so it is not applicable to those sites where the water level is perennially high. A key objective for future work should be the development of techniques capable of measuring the size of material below the water surface.

Acknowledgements

The work was supported by the Leverhulme Trust and Loughborough University. The Countryside Council for Wales, the Tweed Foundation and several individual landowners are thanked for permission to access field sites. Assistance in the field was provided by Tom Buffin-Bélanger, Ian Dennis, Georgina Endfield, Julian Green, Helen Greenwood, Phillippa Noble and Alistair Rennie. Barry Kenny and Natasha Todd-Burley provided laboratory assistance. Celso Garcia undertook much of the initial ‘proof of concept’ image processing work. The paper has benefited from discussions with Rob Ferguson and the insightful and generous comments of Stuart Lane and two other anonymous referees.

References

Adams, J. (1979), Gravel size analysis from photographs, *J. Hydraulics Division, ASCE, 105,* 1247-1255.

Alshibli, K. A., and M. I. Alsaleh (2004), Characterizing surface roughness and shape of sands using digital microscopy, *J. Comput. Civ. Eng., 18,* 36-45.

Bankman, I. N. (Ed.) (2000), *Handbook of Medical Imaging: Processing and Analysis,* 901 pp., Academic Press, London.

Bunte, K., and S. R. Abt (2001), Sampling frame for improving pebble count accuracy in coarse gravel-bed streams, *J. Am. Water Resour. Assoc., 37,* 1001-1014.

Butler, J. B., S. N. Lane, and J. H. Chandler (2001), Automated extraction of grain-size data from gravel surfaces using digital image processing, *J. Hydraul. Res., 39,* 519-529.

Carbonneau, P. E., S. N. Lane, and N. E. Bergeron (2004), Catchment-scale mapping of surface grain size in gravel-bed rivers using airborne digital imagery, *Water Resour. Res., 40,* W07202, doi:10.1029/2003WR002759.

Church, M., D. McLean, and J. F. Wolcott (1987), River bed gravels: sampling and analysis, in *Sediment Transport in Gravel Bed Rivers,* edited by C. R. Thorne, J. C. Bathurst and R. W. Hey, pp. 43-79, Wiley, Chichester.

Diepenbroek, M., A. Bartholoma, and H. Ibbeken (1992), How round is round - a new approach to the topic roundness by Fourier grain shape-analysis, *Sedimentology, 39,* 411-422.

Diepenbroek, M., and C. De Jong (1994), Quantification of textural particle characteristics by image analysis of sediment surfaces – examples from active and paleo-surfaces in steep, coarse-grained mountain environments, in *Dynamics and Geomorphology of Mountain Rivers,* edited by P. Ergenzinger and K. H. Schmidt, pp. 301-314, Springer-Verlag, Berlin.

Dymond, J. R., and C. M. Trotter (1997), Directional reflectance of vegetation measured by a calibrated digital camera, *Appl. Opt., 36,* 4314-4319.

Franciskovic-Bilinski, S., H. Bilinski, N. Vdovic, Y. Balagurunathan, and E. R. Dougherty (2003), Application of image-based granulometry to siliceous and calcareous estuarine and marine sediments, *Estuar. Coast. Shelf Sci., 58,* 227-239.

Ghalib, A. M., and R. D. Hryciw (1999), Soil particle size distribution by mosaic imaging and watershed analysis, *J. Comput. Civ. Eng., 13,* 80-87.

Graham, D. J., I. Reid, and S. P. Rice (2005), Automated sizing of coarse-grained sediments: image-processing procedures, *Math. Geol., 37,* 1-28.

Green, J. C. (2003), The precision of sampling grain-size percentiles using the Wolman method, *Earth Surf. Process. Landforms, 28,* 979-991.

Ibbeken, H., and R. Schleyer (1986), Photo-sieving - a method for grain-size analysis of coarse-grained, unconsolidated bedding surfaces, *Earth Surf. Process. Landforms, 11,* 59-77.

Ibbeken, H., D. A. Warnke, and M. Diepenbroek (1998), Granulometric study of the Hanaupah Fan, Death Valley, California, *Earth Surf. Process. Landforms, 23,* 481-492.

Kellerhals, R., and D. I. Bray (1971), Sampling procedures for coarse fluvial sediments, *J. Hydraulics Division, ASCE, 97,* 1165-1180.

Lane, E. W., and E. J. Carlson (1953), Some factors affecting the stability of canals constructed in coarse granular material, *Proceedings of the 5th IAHR Congress,* 37-48.

Marcus, W. A., S. C. Ladd, and J. A. Stoughton (1995), Pebble counts and the role of user-dependent bias in documenting sediment size distributions, *Water Resour. Res., 31,* 2625-2631.

McEwan, I. K., T. M. Sheen, G. J. Cunningham, and A. R. Allen (2000), Estimating the size composition of sediment surfaces through image analysis. *Proc. Inst. Civil Eng. - Water Marit. Energy, 142,* 189-195.

Perring, C. S., S. J. Barnes, M. Verrall, and R. E. T. Hill (2004), Using automated digital image analysis to provide quantitative petrographic data on olivine-phyric basalts, *Comput. Geosci., 30,* 183-195.

Posadas, A. N. D., D. Gimenez, R. Quiroz, and R. Protz (2003), Multifractal characterization of soil pore systems, *Soil Sci. Soc. Am. J., 67,* 1361-1369.

Reid, I., S. Rice, and C. Garcia (2001), Discussion of “The measurement of gravel-bed river morphology”, in *Gravel-Bed Rivers V,* edited by M. P. Mosley, pp. 325-327, New Zealand Hydrological Society, Wellington.

Rice, S., and M. Church (1998), Grain size along two gravel-bed rivers: statistical variation, spatial pattern and sedimentary links, *Earth Surf. Process. Landforms, 23,* 345-363.

Rice, S., and M. Church (1996), Sampling surficial fluvial gravels: the precision of size distribution percentile estimates, *J. Sediment. Res., 66,* 654-665.

Russ, J. C. (1999), *The Image Processing Handbook,* 3rd ed., 771 pp., CRC Press, Boca Raton, Florida.

Schenk, T. (1999), *Digital Photogrammetry.* Vol. 1. 1st ed., 428 pp., TerraScience, Laurelville, Ohio.

Sime, L. C., and R. I. Ferguson (2003), Information on grain sizes in gravel-bed rivers by automated image analysis, *J. Sediment. Res., 73,* 630-636.

Wettimuny, R., and D. Penumadu (2004), Application of Fourier analysis to digital imaging for particle shape analysis, *J. Comput. Civ. Eng., 18,* 2-9.

Wolcott, J., and M. Church (1991), Strategies for sampling spatially heterogeneous phenomena - the example of river gravels, *J. Sediment. Petrol., 61,* 534-543.

Wolf, P. R., and B. A. Dewitt (2000), *Elements of Photogrammetry,* 3rd ed., 608 pp., McGraw-Hill, Boston.

Wolman, M. G. (1954), Method of sampling coarse river bed material, *Trans. AGU, 35,* 951-956.

Zhang, Z. (2000), A flexible new technique for camera calibration, *IEEE Trans. Pattern Anal., 22,* 1330-1334.

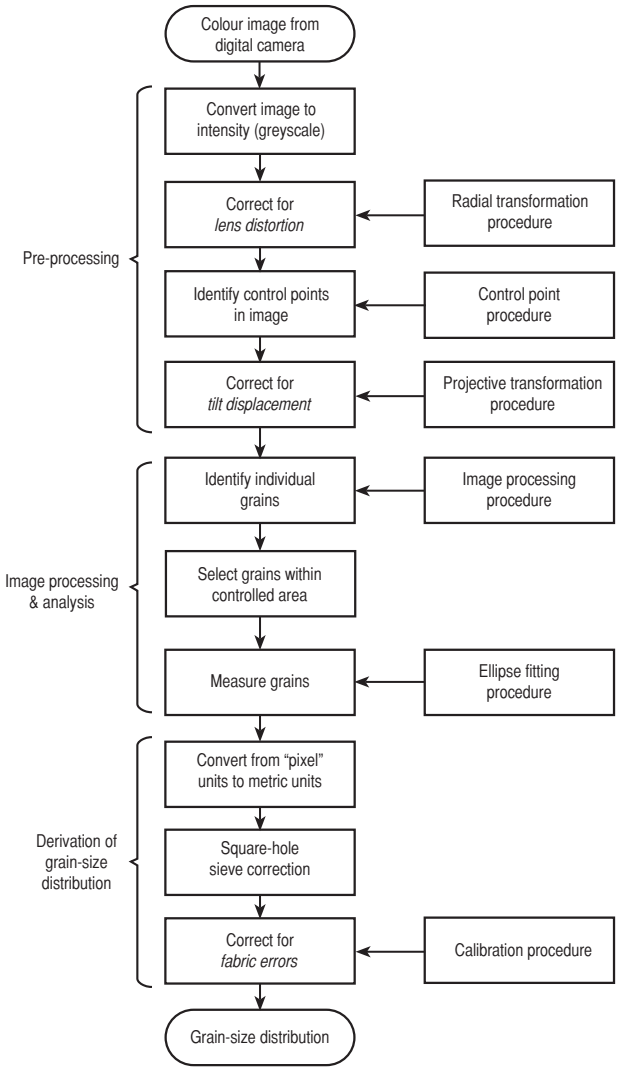

Figure 1. The stages required to extract grain-size data from a digital image [reproduced with permission from *Graham et al.,* 2005].

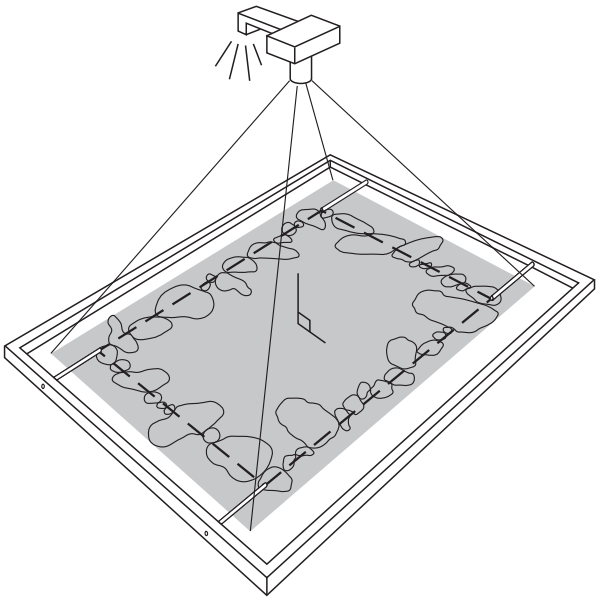

Figure 2. Illustration of the recommended photographic procedure. An oversized frame with protruding metal wires defines the corners of the sampling patch. The photographed area (shaded) must include all grains intersecting the patch edge (pecked outline). The photograph is taken approximately vertically with a hand-held digital camera whilst the patch is shielded from direct sunlight and lit with a camera-mounted flash.

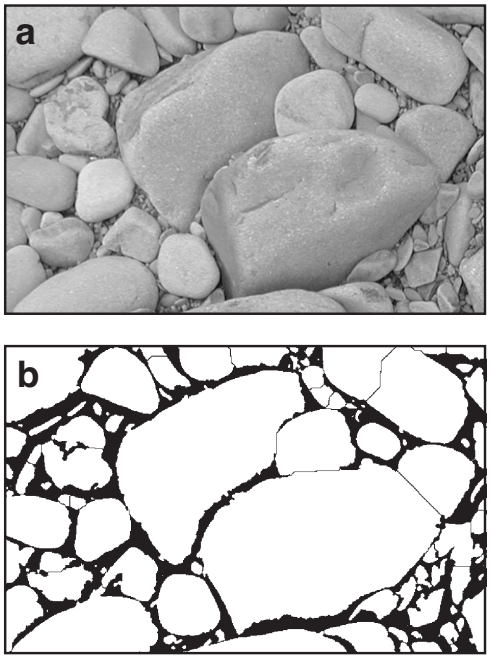

Figure 3. Illustration of the results of the image-processing procedure. (a) Extract from a digital photograph of a natural sediment surface. (b) The same image after the application of the optimal image-processing processing procedure described in section 2.3.

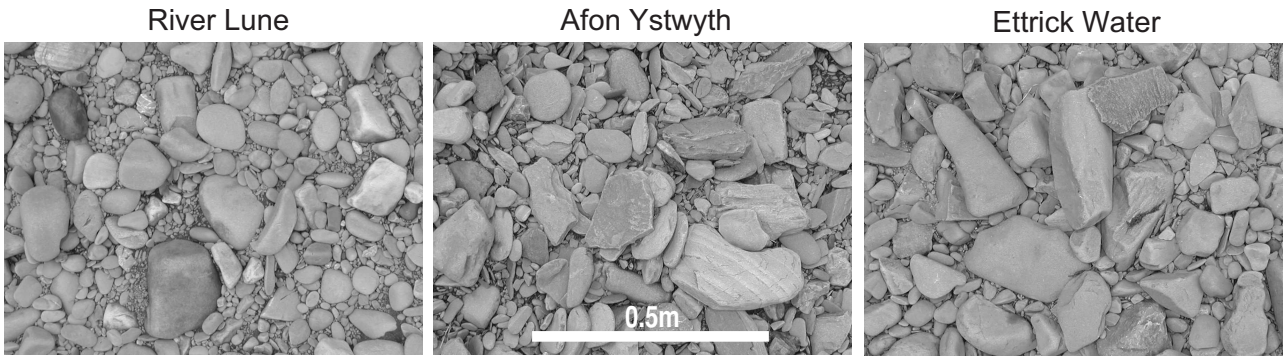

Figure 4. Photographs illustrating the variation in grain shape, roundness and fabric at each of the three lithologically-differentiated field sites.

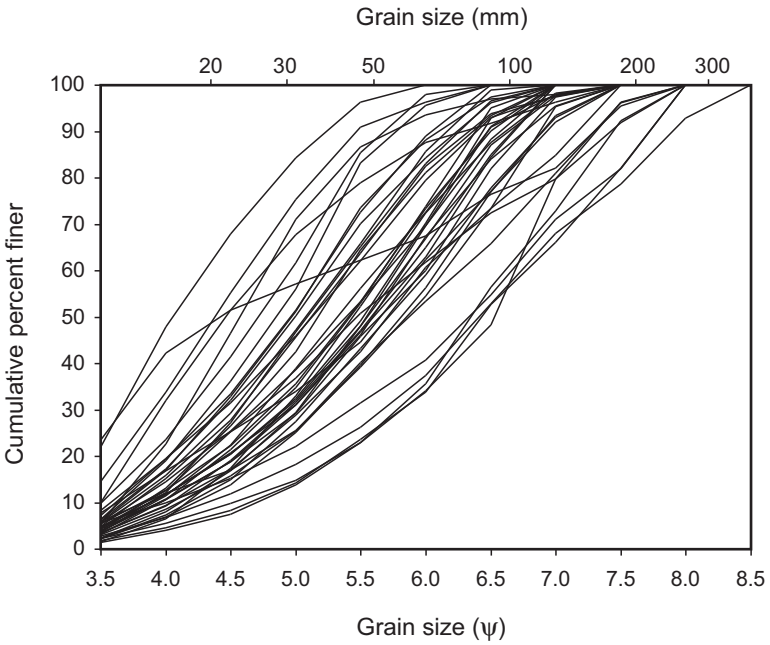

Figure 5. Cumulative grain-size distribution curves for the 39 sediment patches showing the range of textures in the bed material used to test the image-processing procedure. Data are for area-by-number distributions (paint-and-pick samples) truncated at 3 ψ (8 mm) and converted to grid-by-number using the method of *Kellerhals and Bray* [1971].

Figure 6. Photographic illustration of the methods by which the test data were collected. A simpler procedure (Figure 2) is recommended for routine data collection. (a) To collect the test images, a camera is held by a tripod head mounted on a horizontal metal bar and suspended between two tripods. A wooden frame has been laid over the sample patch to define the area for spray-painting. A fabric skirt minimizes drifting of paint onto adjacent grains. (b) A sample patch during paint-and-pick sampling. Every painted grain with a *b*-axis greater than 4 mm is collected and returned to the laboratory for grading.

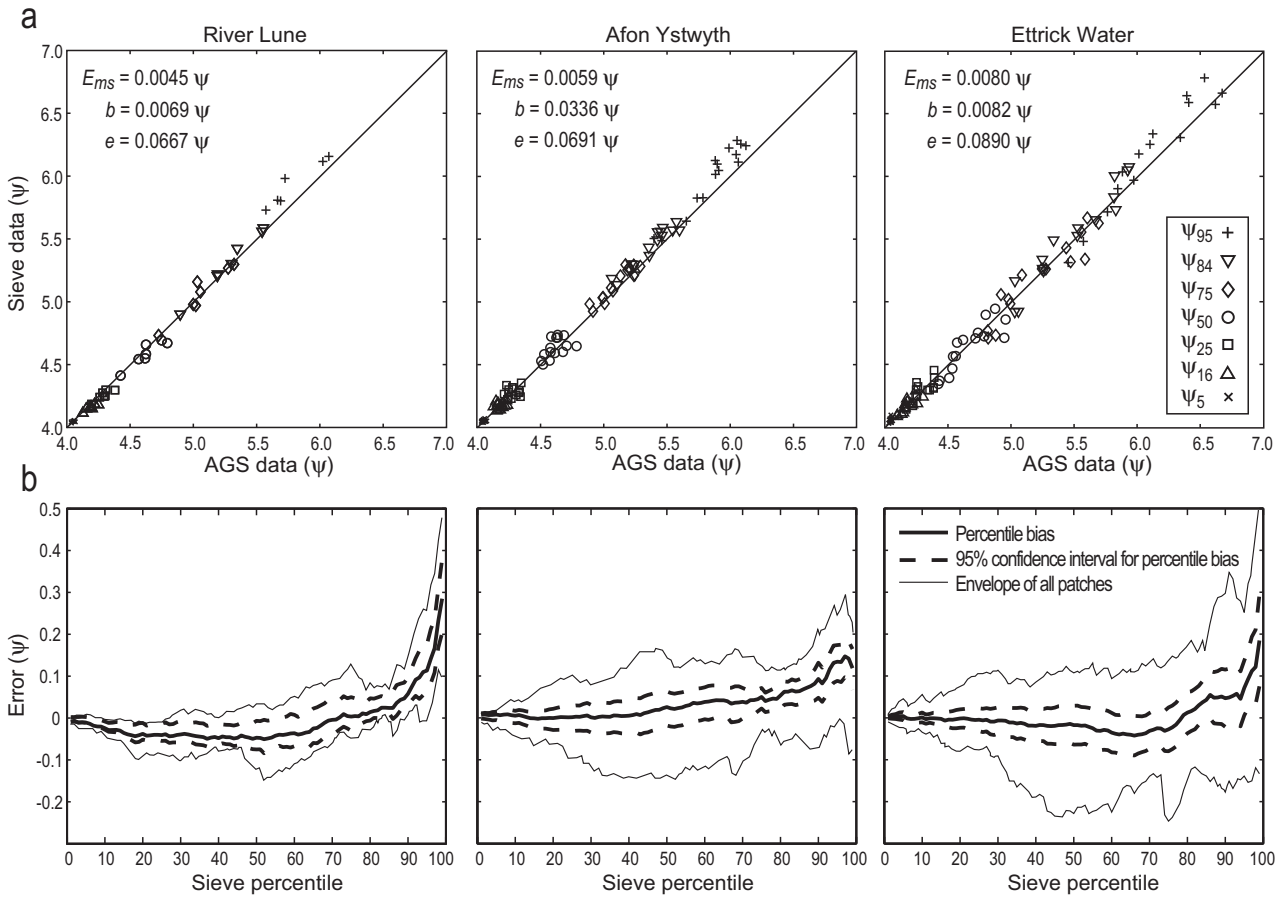

Figure 7. Performance of the automated grain-sizing (AGS) procedure on an area-by-number basis. (a) Grain size at specified percentiles of the size distribution as defined by the sieve and AGS procedures for each of the patches, grouped by field site. Mean square error E_{ms}, procedure bias b, and irreducible random error e are quoted for each site. (b) Envelopes for the error in grain size determined by the AGS procedure at each integer percentile from 1 to 99, grouped by field site. The heavy solid and dashed lines represent the bias for each percentile and 95% confidence for the population percentile bias, respectively.

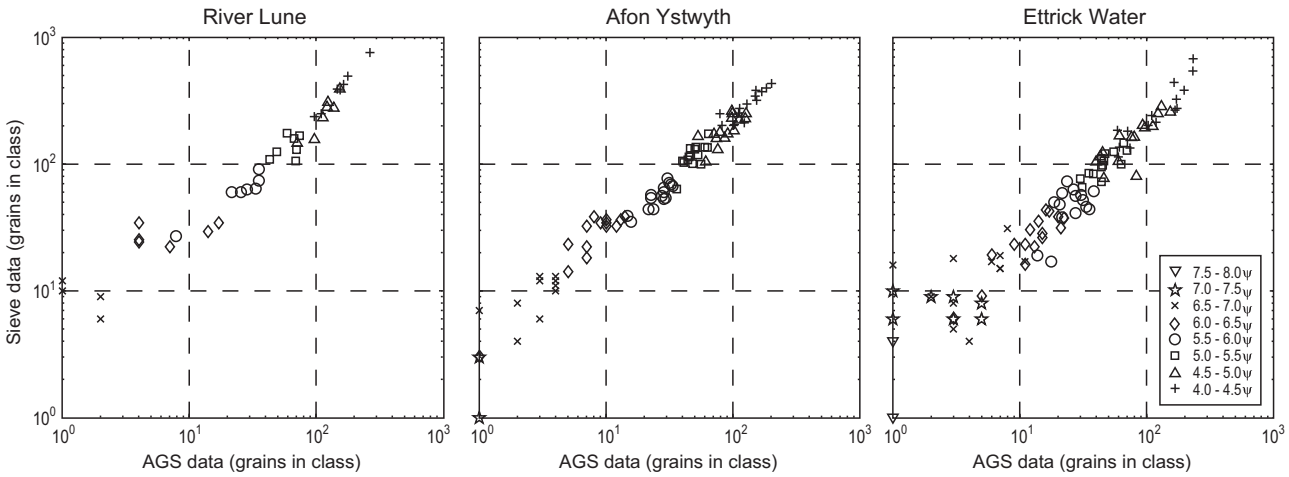

Figure 8. The relation between the number of grains in 0.5 ψ size classes using the AGS procedure and the paint-and-pick derived sieve data for each of the three field sites.

Table 1. Summary properties of the bed-material patches for each of the rivers.

	Number of patches	Sample size (grains per patch)			ψ_{95} (and D_{95} in mm)			ψ_{50} (and D_{50} in mm)			Sorting (ψ)		
		Min / max	Mean	Std. Dev.	Min / max	Mean	Std. Dev.	Min / max	Mean	Std. Dev.	Min / max	Mean	Std. Dev.
River Lune	7	609 / 1310	908	247	6.17 / 6.98 (72 / 126)	6.60 (99)	0.28 (19)	4.57 / 5.60 (24 / 48)	5.20 (38)	0.37 (9)	0.79 / 1.08	0.95	0.09
Afon Ystwyth	16	458 / 901	677	137	5.43 / 7.13 (43 / 140)	6.52 (96)	0.46 (27)	4.05 / 5.72 (17 / 53)	5.27 (40)	0.45 (10)	0.75 / 1.27	0.96	0.12
Ettrick Water	16	275 / 1113	619	228	5.84 / 8.10 (57 / 274)	7.19 (158)	0.62 (60)	4.38 / 6.53 (21 / 93)	5.60 (54)	0.75 (25)	0.82 / 1.60	1.15	0.20

Note: Data are for area-by-number distributions (paint-and-pick samples) truncated at 3 ψ (8 mm) and converted to grid-by-number using a *Kellerhals and Bray* [1971] transformation. Sorting is *Folk and Ward* [1957] inclusive, truncated at 3 ψ.

Table 2. Mean grain flatness and associated square-hole sieve correction factors [*Church et al.*, 1987] for each of the three field sites.

	Mean flatness *(c/b)*	Square-hole sieve correction factor *(D_s/b)*
River Lune	0.51	0.79
Afon Ystwyth	0.44	0.77
Ettrick Water	0.58	0.82

Table 3. Percentile bias and standard error for each of seven commonly-used percentiles at each field site. Data are for area-by-number distributions. Biases that are not significantly different from zero (95% confidence) are italicized.

	River Lune		Afon Ystwyth		Ettrick Water	
	Percentile bias (ψ)	Std. error (ψ)	Percentile bias (ψ)	Std. error (ψ)	Percentile bias (ψ)	Std. error (ψ)
ψ_5	*-0.0043*	0.0034	*0.0014*	0.0032	*0.0041*	0.0047
ψ_{16}	-0.0326	0.0076	*-0.0079*	0.0085	*-0.0064*	0.0090
ψ_{25}	-0.0343	0.0102	*-0.0056*	0.0127	*-0.0045*	0.0136
ψ_{50}	-0.0407	0.0170	*0.0172*	0.0177	*-0.0173*	0.0232
ψ_{75}	*0.0098*	0.0201	*0.0375*	0.0117	-0.0273	0.0261
ψ_{84}	0.0312	0.0089	*0.0485*	0.0144	0.0374	0.0252
ψ_{95}	0.1196	0.0282	0.1113	0.0245	0.0712	0.0328

Table 4. Comparative performance of the *Sime and Ferguson* [2003] and automated grain-sizing (AGS) procedures on a grid-by-number basis.

	Published method of *Sime and Ferguson* [2003]			Corrected method of *Sime and Ferguson* [2003]			AGS method presented here		
	Mean square error, E_{ms} (ψ)	Bias, b (ψ)	Irreducible random error, e (ψ)	Mean square error, E_{ms} (ψ)	Bias, b (ψ)	Irreducible random error, e (ψ)	Mean square error, E_{ms} (ψ)	Bias, b (ψ)	Irreducible random error, e (ψ)
River Lune	0.28	-0.46	0.26	0.03	0.05	0.15	0.07	0.17	0.19
Afon Ystwyth	0.37	-0.56	0.23	0.03	0.06	0.15	0.02	0.10	0.11
Ettrick Water	0.15	-0.23	0.32	0.22	0.30	0.35	0.07	0.16	0.22
Mean	0.27	-0.42	0.27	0.09	0.14	0.22	0.05	0.14	0.18